Solar Energy Materials & Solar Cells 92 (2008) 1236–1240

Contents lists available at ScienceDirect

Solar Energy Materials & Solar Cells

journal homepage: www.elsevier.com/locate/solmat

A TEM study of SiC particles and filaments precipitated in multicrystalline Si for solar cells

A. Lotnyk *, J. Bauer, O. Breitenstein, H. Blumtritt

Max Planck Institute of Microstructure Physics, Weinberg 2, D-06120 Halle, Germany

ARTICLE INFO

Article history:
Received 22 February 2008
Received in revised form
18 April 2008
Accepted 18 April 2008
Available online 5 June 2008

Keywords:
Multicrystalline silicon (mc-Si)
Solar cell
SiC
Transmission electron microscopy (TEM)

ABSTRACT

The microstructure of SiC particles and SiC filament-type precipitates found in block-cast multicrystalline Si was studied in detail by transmission electron microscopy (TEM). TEM investigations showed that the SiC particles are single crystalline and the SiC filaments are microcrystalline. Both types of precipitates consist of cubic SiC. However, a high density of planar defects was found in the filaments. Very wavy and rough interface between SiC filaments and silicon (Si) was revealed by high-resolution TEM. In addition, SiC filaments do not show a special orientation relationship with respect to the Si matrix. The growth mechanisms of SiC precipitates are discussed. Finally, the influence of SiC inclusions in terms of device performance is considered.

1. Introduction

Silicon (Si) is the most commonly used material for the production of solar cells. The cells can be made from single-crystalline Si (c-Si), multicrystalline Si (mc-Si) or amorphous Si (α-Si). Particularly, mc-Si is today's dominant material in solar cell industry due to its low cost compared to c-Si cells and its rather high efficiency compared to α-Si cells.

Low-cost mc-Si is mostly fabricated by a vertical freezing process [1]. In this process, mc-Si is molten in a crucible (approx. 200 kg) and is then slowly crystallized from bottom to top. Afterwards, these blocks are sliced into wafers for solar cell fabrication. The casting crucibles are made from quartz material which is covered by silicon nitride (Si_3N_4). The melting of mc-Si ingot is performed by graphite heaters in an inert gas atmosphere. During processing of block-cast mc-Si, SiC precipitates appear frequently in the top part of mc-Si blocks. There are two different types of SiC precipitates: (1) clusters of SiC particles (several tens of micrometers in size) mostly occurring on Si_3N_4 rods [2–11] and (2) SiC filaments mostly growing at grain boundaries of mc-Si [4–8]. The filaments have a size of several micrometers in diameter and of several hundred micrometers or even millimeters in length and grow in upward direction [5]. The SiC precipitates have already been well characterized by scanning electron microscopy (SEM), energy dispersive X-ray spectroscopy (EDX), IR-transmission microscopy, lock-in thermography (LIT), X-ray fluorescence and electron/light beam-induced current methods [3–5,8,12]. However, due to the complexity of specimen preparation, only few reports were devoted to TEM characterization [4,13]. It is well known that the different thinning rate in two phase materials, e.g. SiC embedded in mc-Si, is a common problem in the samples preparation for TEM investigation by conventional methods. This often leads to samples in which one phase is evenly polished while another phase is either etched out or stands proud of the surrounding material. This problem can be overcome by using focused ion-beam (FIB) in the preparation [14]. In addition, the most attractive feature of the FIB technique is its ability to accurately cut a TEM specimen at the area of interest.

Recently, the electrical properties of SiC precipitates found in mc-Si for solar cells were reported [8,13]. It was found that SiC filaments may cause strong shunts in the cells causing degradation in the performance. The aim of the current study is to investigate in detail the microstructure and modifications of SiC particles and filaments by TEM. The crystallographic orientations between SiC filaments and the Si matrix as well as the cross-section of the interface between the filaments and the matrix are also investigated. The samples for TEM investigations were prepared by FIB.

2. Experimental

The samples studied in this work were commercial solar cells fabricated from block-cast mc-Si. The areas of interest were found by LIT shunt imaging over complete solar cells as described in

* Corresponding author. Tel.: +49 345 5582 692; fax: +49 345 5511223.
E-mail address: lotnyk@mpi-halle.de (A. Lotnyk).

0927-0248/$ - see front matter © 2008 Elsevier B.V. All rights reserved.
doi:10.1016/j.solmat.2008.04.016

Refs. [7,8]. Figs. 1(a) and (b) show typical SEM images of clusters of SiC particles and SiC filaments, respectively. In some cases, between 10% and 15% of solar cells of one batch may contain shunts caused by SiC inclusions. The elemental composition of SiC filaments was proven by EDX analysis [13]. It should be noted that the SiC filaments were not found by authors in Refs. [2,9–11] who also used commercial solar cells in their investigations. We believe that this is mainly due to dissolution technique used in their works for isolation of SiC and Si_3N_4 inclusions from bulk Si. Many losses and damages of the inclusions occur during filtration process and especially during mechanical removing of the precipitates from the paper filter, as was mentioned in Refs. [8,11]. The method is well suitable for the identification of big SiC and Si_3N_4 particles (several tens of micrometers in diameter). However, this method cannot be applied in the identification of SiC filaments, which are one order or more of magnitude smaller. In order to dissolve SiC filaments without their destruction and loss, a method developed in Ref. [8] should be applied. In the present work, we did not dissolve completely SiC filaments from bulk Si. Thus, they are still embedded in bulk Si and stick out of the material. Moreover, in our work the areas containing shunts were found before preparation by LIT shunt imaging of the cells [7,8]. In this way, we regularly found the same type of SiC filaments in the shunt regions of solar cells produced by different manufacturers [7]. Note that LIT was not used in Refs. [2,9–11].

Cross-sectional and plan-view specimens for TEM investigations were prepared by FIB milling using a 'lift-out' technique. A FEI Nova 600 NanoLab system equipped with micromanipulator was used for this work. To produce a plan-view sample a FIB lamella was cut parallel to the area of interest. To prepare a cross-sectional specimen a FIB lamella was cut perpendicular to the area of interest. Two types of cross-sectional specimens were prepared for the SiC filaments lying in grain boundaries of mc-Si. One type of cross-section was cut parallel to a grain boundary (the direction of cutting is shown by arrow '*A*' in Fig. 1(b)) whereas another type of cross-section was cut perpendicular to a grain boundary (the direction of cutting is shown by arrow '*B*' in Fig. 1(b)). TEM investigations were carried out in a conventional TEM CM 20 Twin (Philips, Netherlands) at a primary beam energy of 200 keV, and in a HRTEM JEOL 4010 (JEOL, Japan) at a primary beam energy of 400 keV. The CM 20 Twin microscope is equipped with a double-tilt specimen holder. The holder allows tilts of $\pm 45^\circ$.

3. Results

There are many different polytypes of SiC [15]. The polytypes arise from different periodic (stacking) sequence of tetrahedrally bonded Si-C bilayers. Identification of the polytype of SiC particles and SiC filaments precipitated in block-cast mc-Si was performed by the most adopted TEM methods, namely from SAED patterns taken from a set of crystallographic directions and HRTEM images recorded along a low-index zone axis.

3.1. Characterization of SiC particles

Fig. 2(a) shows a cross-sectional bright field TEM image of a SiC particle formed in mc-Si. Figs. 2(b) and (c) present two SAED patterns along two different zone axes of Fig. 2(a). The patterns were indexed as [1 0 1] and [0 0 1] zone axes of cubic SiC (3C polytype, $a = 0.435$ nm, space group $F\bar{4}3m$), respectively. The angle between zone-axis patterns (Fig. 2(b) and (c)) read from the tilting angle of the TEM specimen holder is $45 \pm 1^\circ$, in good agreement with 45° estimated from a stereographic projection for cubic 3C-SiC. It should be noted that the characterization of SiC particles in mc-Si by electron back scatter diffraction [11] and by X-ray diffraction [9] showed also the cubic structure of SiC particles. In addition, SAED investigations of the SiC particle showed that the particle is single crystalline. However, macroscopic defects like cracks were observed within the particles. No other defects have been found up to now in these SiC particles.

3.2. Characterization of SiC filaments

Fig. 3(a) shows a typical plan-view bright field TEM image of a SiC filament embedded in a grain boundary of mc-Si. Figs. 3(b) and (c) present two SAED patterns along [1 0 1] and [1 1 2] zone axes, respectively, of the region marked in Fig. 3(a). The patterns were indexed using the cubic unit cell of 3C-SiC. The angle between zone-axis patterns (Fig. 3(b) and (c)) read from the tilting angle of the TEM specimen holder is $28 \pm 1^\circ$, reasonable close to 30° calculated from a stereographic projection for cubic 3C-SiC. TEM investigations in dark and bright field of the several SiC filaments showed that the filaments are microcrystalline and consist of several parts (Fig. 3(a)). No accumulation of dislocations was found in the Si matrix around the filaments.

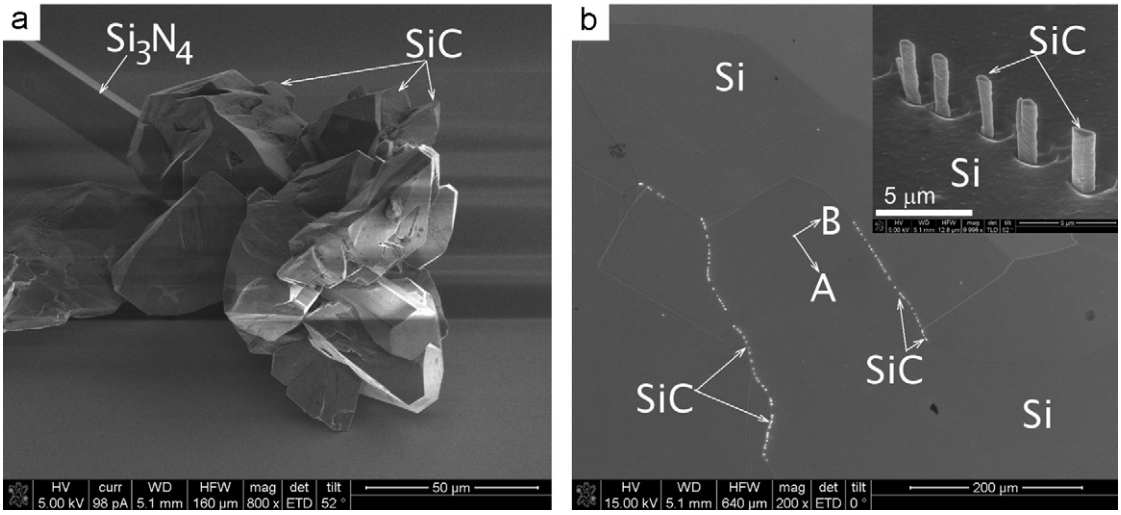

Fig. 1. (a) SEM image of cluster of SiC particles growing on Si_3N_4 rod. (b) SEM image of SiC filaments embedded in grain boundaries of mc-Si (see also inset in (b)). The arrows '*A*' and '*B*' in image (b) show the directions of cutting used in the preparations of cross-sectional samples for TEM by FIB. The arrow '*A*' corresponds to the direction parallel to a grain boundary of mc-Si while the arrow '*B*' corresponds to the direction perpendicular to a grain boundary of mc-Si (see also text).

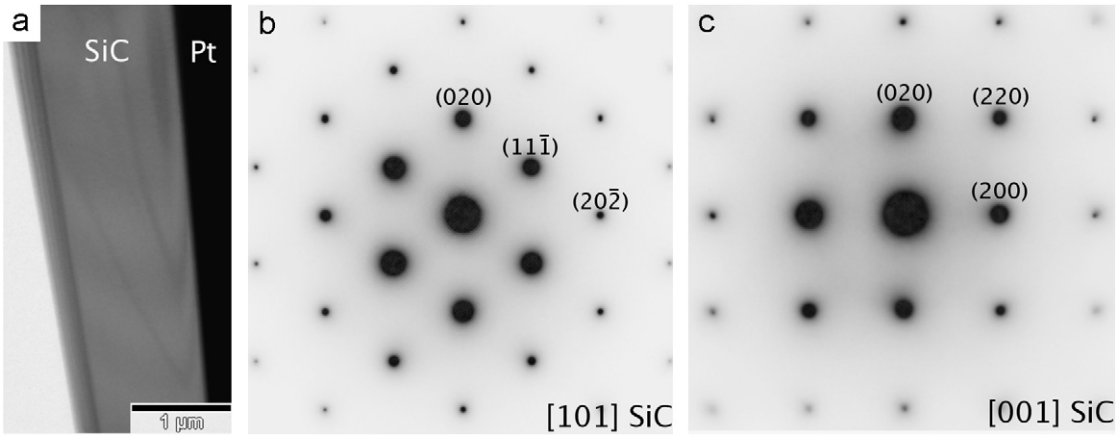

Fig. 2. (a) Cross-section bright field TEM image of SiC particle and (b) and (c) SAED patterns of SiC particle taken along two different zone axes. The Pt layer seen in (a) is due to FIB sample preparation.

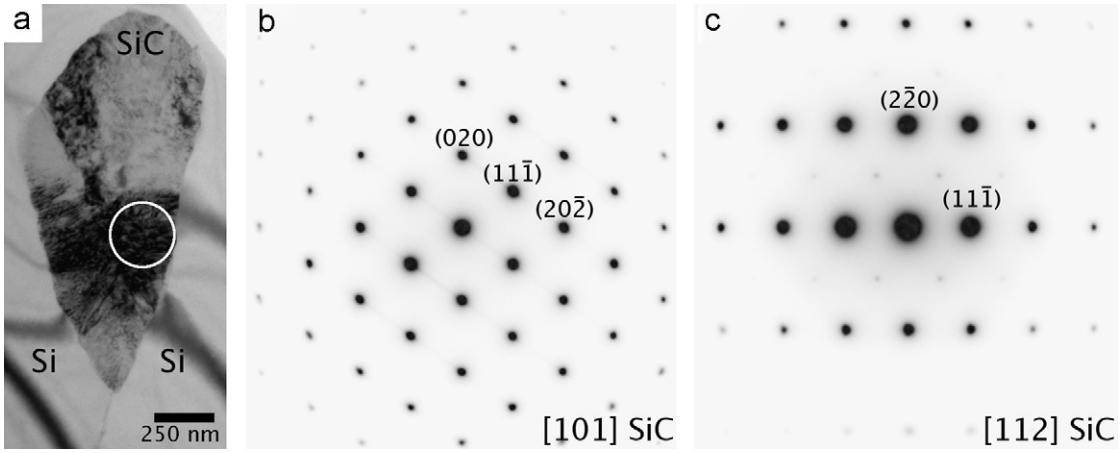

Fig. 3. (a) Plan-view bright field TEM image of SiC filament embedded in a grain boundary of mc-Si and (b) and (c) SAED patterns of SiC filament recorded along two different zone axes. The patterns were taken from the region marked in (a).

In order to check the presence of other polytypes of SiC in the filaments, SAED and HRTEM studies were performed on a cross-sectional sample cut along a grain boundary of mc-Si. Fig. 4(a) shows a typical bright field TEM image of SiC filaments embedded in a grain boundary of mc-Si. The TEM sample was cut parallel to a grain boundary. SAED investigations performed on the cross-sectional sample containing several filaments proved that the filaments consist of the 3C-SiC. However, the filaments contain a high density of planar defects (Fig. 4(b)) such as stacking faults and twins (Fig. 4(c)). An SAED pattern recorded from representative region is shown in Fig. 4(d). The SAED image shows weak diffuse streaks along $\langle 111 \rangle$ directions of cubic SiC, indicating the presence of stacking faults (see also Fig. 3(b)). The formation of defects is due to the large lattice mismatch between Si and 3C-SiC (19.9%). In addition, Fig. 4(d) contains extra reflections in one-third and two-thirds of the (111) SiC reflection, indicating a threefold periodicity. HRTEM investigations showed that the regions with threefold periodicity were always associated with {111} twin regions of cubic SiC (not shown). Similar regions were also found in other parts of the TEM sample. Previously, it was reported that the threefold periodic structure presented in SAED pattern or in the HRTEM image of cubic SiC is due to overlapping of twinned cubic SiC domains [16,17]. No indication for the presence of other polytypes of SiC was found by both SAED and HRTEM investigations.

Fig. 5 shows a cross-section HRTEM image of the sample cut perpendicular to a grain boundary of mc-Si. The interface between SiC and Si matrix is rough and very wavy. HRTEM (see Fig. 5) and SAED investigations showed also that SiC filaments did not have a special orientation relationship with respect to the Si matrix.

4. Discussion

SiC occurs mainly in two modifications, namely as α-SiC with hexagonal structure and as β-SiC with cubic structure. However, the α-SiC has many polytypes [15]. In the present work, we identify only the β-modification of SiC without the presence of other polytypes of SiC. According to the thermodynamic data, the β-SiC has lower Gibbs energy of formation compared to the α-SiC (ranging from -67.633 to -59.629 kJ/mol at temperatures between 700 and 1700 K for β-SiC and ranging from -65.866 to -57.665 kJ/mol at temperatures between 700 and 1700 K for α-SiC) [18] and, thus, should be the most stable modification. However, the stability difference is actually small. Consequently, thermodynamics cannot explain why only the β-SiC precipitates in mc-Si solar material. Previously, it was shown that donors like nitrogen favor the formation of cubic SiC [19]. The precipitated SiC in mc-Si is n-doped by nitrogen [8,20]. The latter can explain the formation of SiC clusters and of SiC filaments with cubic structure

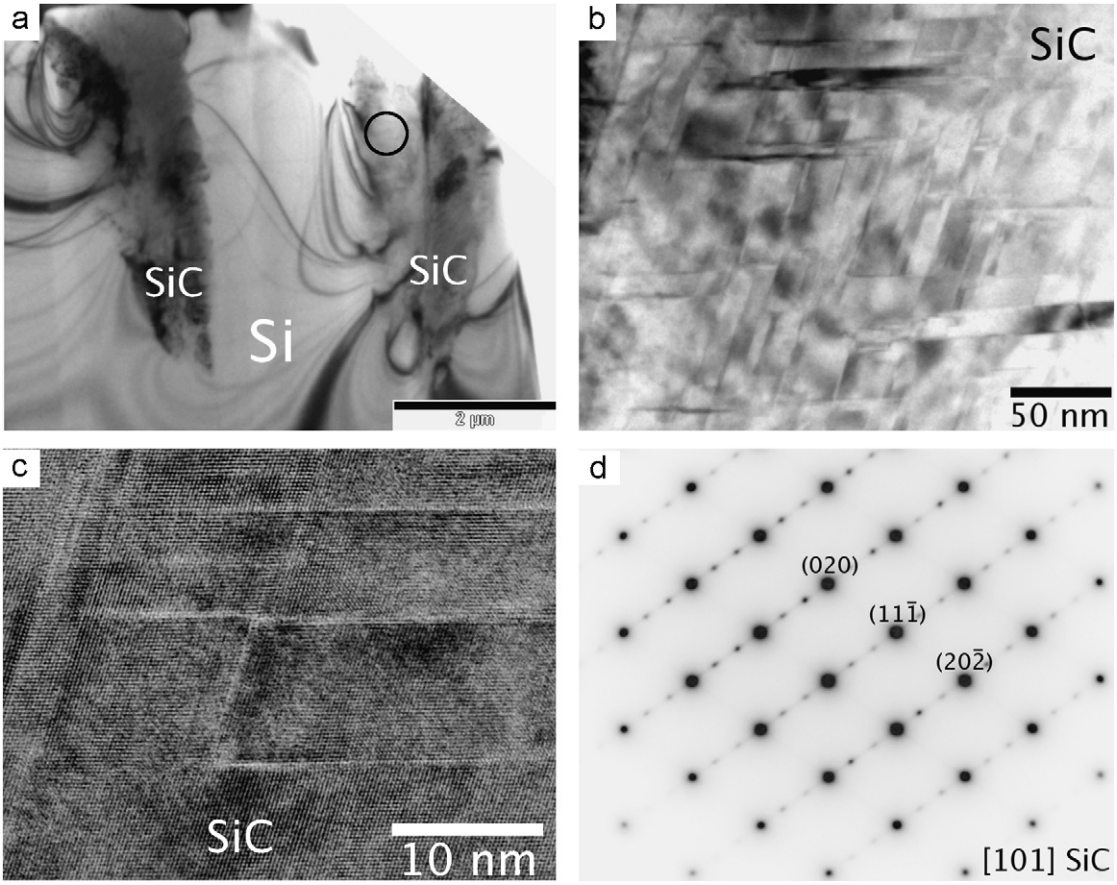

Fig. 4. (a) Cross-section bright field TEM image of SiC filaments embedded in a grain boundary of mc-Si. (b) Bright field TEM micrograph of the region marked in (a). The micrograph points out the high density of defects in SiC filament. (c) HRTEM image showing planar defects in SiC filament. (d) SAED pattern of SiC filament taken from the region marked in (a). This TEM sample was cut along a grain boundary of mc-Si (see arrow '*A*' in Fig. 1(b)).

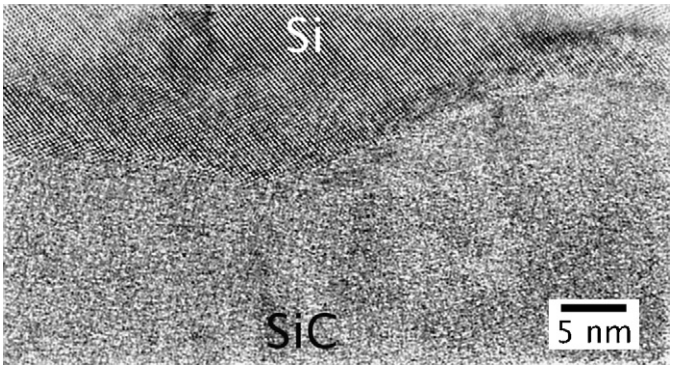

Fig. 5. HRTEM image of Si–SiC interface. The image shows that the interface is rough and very wavy. In addition, there is no well-defined orientation relationship between Si and SiC. Viewing direction is [101] Si. This TEM sample was cut perpendicular to a grain boundary of mc-Si (see arrow '*B*' in Fig. 1(b)).

(β-modification) observed in the current study. It should be noted that the presence of nitrogen in mc-Si is evidenced by the precipitation of Si_3N_4. The latter is frequently observed in mc-Si [2–11,20].

The formation of SiC precipitates in mc-Si is obviously due to carbon contamination of the Si melt, which is probably caused by the graphite heaters in the high-temperature furnace [21]. We found that the microstructure of SiC particles is very different compared to the microstructure of SiC filaments. The particles are single crystalline while the filaments are microcrystalline with a high density of planar defects. Consequently, we can assume different growth mechanisms of SiC particles and of SiC filaments. Below, we describe the possible formation mechanisms of SiC particles and of SiC filaments.

The single-crystalline form of SiC particles suggests that the particles are growing in the Si melt. Also SiC particles in mc-Si are frequently precipitated around Si_3N_4 rods [6–8,10,11], which are completely formed in the melt [6,10,11]. This is an additional argument that the formation of SiC particles occurs in the silicon melt. Previously, epitaxial β-SiC films were produced on Si substrates covered by Si_3N_4 buffer layers [22]. This fact can explain the precipitation of SiC particles around Si_3N_4 rods in the Si melt and the rods can act as nucleation sites for the formation of SiC particles. Thus, the nucleation of SiC particles is heterogeneous (see also below). In contrast, SiC filaments are microcrystalline and, thus, their growth mechanism is different from the particles' one. In many examples of nucleation in solids it is found that the nucleation of new compounds is heterogeneous [23]. Defects in solids like grain boundaries, grain edges, dislocations, stacking faults, etc., act as heterogeneous sites for nucleation. Analysis of the nucleation of incoherent precipitates on grain boundaries and on dislocations shows that the nucleus forms on the pre-existing defect. Therefore, the energy of formation of the nucleus is reduced by that proportion of the defect energy that is consumed by the nucleus as it is formed [23]. Thus, the defects are favorable sites for precipitation. The SiC filaments are frequently precipitated in grain boundaries of mc-Si [4–8], indicating heterogeneous nucleation of the SiC filaments. In this case, grain boundaries of Si act as nucleation sites for the

formation of filaments. Consequently, the growth of SiC filaments may start during crystallization of Si by diffusion of carbon from the melt into pre-forming grain boundaries of Si, or the formation of SiC filaments in mc-Si may occur by solid-state diffusion of dissolved carbon in the solid Si into pre-existing Si grains. Further work is required to draw more precise conclusions on the mechanism of the formation of SiC filaments.

Now, we would like to discuss the influence of SiC inclusions in terms of device performance. In the starting material, the SiC filaments have a length up to several hundreds micrometers or even several millimeters [5]. The filaments are growing in crystallization direction of mc-Si. Thus, the filaments can go through several solar cell wafers and are electrically connected both with emitter and the back contact of the solar cells. Consequently, the filaments may cause strong ohmic (linear) shunts in the cells [8,20], and thus decrease the efficiency of the cells. Depending on the degree of shunting, the absolute efficiency measured under standard conditions ($1000\,W/m^2$, $25\,^{\circ}C$) may be reduced by these SiC-induced shunts by ~0.5–1.5%. However, this degradation can be even higher reaching up to 5% if the cell is working at reduced light intensity, as it is often the case in middle Europe [24]. On the other hand, SiC particles are lying isolated in the mc-Si material and are not expected to cause any shunts in the cells, as long as their size does not exceed the thickness of the solar cell.

5. Conclusions

The microstructure of SiC particles and SiC filaments occurring in mc-Si was investigated in detail by TEM. SAED investigations showed that the SiC particles are single crystalline and the SiC filaments are microcrystalline. Both types of precipitates consist of cubic SiC (3C polytype). It is suspected that nitrogen present in mc-Si favors the formation of SiC particles and SiC filaments with cubic structure. A high density of planar defects like stacking faults and twins was found in the SiC filaments. The formation of defects is attributed to the large lattice mismatch between Si and 3C-SiC. Many regions containing a threefold periodic structure were observed within the 3C-SiC filaments, which is due to the overlapping of twinned cubic SiC domains.

Different formation mechanisms of SiC particles and of SiC filaments are assumed. The formation of SiC particles is supposed to grow in the Si melt contaminated by carbon. In contrast, SiC filaments may form during crystallization of Si by diffusion of carbon from the melt into pre-forming grain boundaries of Si. Alternatively, the filaments may also grow by solid-state diffusion of dissolved carbon in the solid Si matrix into already pre-existing Si grains. We are presently working on a precise identification of detailed mechanism of the formation of SiC filaments.

The influence of SiC inclusions in terms of device performance was also discussed. Since SiC filaments may be electrically connected both with emitter and back contact of the solar cell, they may cause strong ohmic shunts [8,20], and thus decrease its efficiency.

Acknowledgments

This work was supported by the Federal Ministry of Environment (BMU) under Contract number 0327650D (Solar Focus). Q-Cells AG (Thalheim, Germany) is gratefully acknowledged for providing the material used for this investigation.

References

[1] A. Luque, S. Hegedus (Eds.), Handbook of Photovoltaic Science and Engineering, Wiley, Chichester, 2003.
[2] A. Ciftja, L. Zhang, T.A. Engh, A. Kvithyld, Purification of solar cell silicon materials through filtration, Rare Metals 25 (2006) 180.
[3] T. Buonassisi, A.A. Istratov, M.D. Pickett, J.-P. Rakotoniaina, O. Breitenstein, M.A. Marcus, S.M. Heald, E.R. Weber, Transition metals in photovoltaic–grade ingot–cast multicrystalline silicon: Assessing the role of impurities in silicon nitride crucible lining material, J. Cryst. Growth 287 (2006) 402.
[4] O. Breitenstein, J.P. Rakotoniana, M.H. Al Rifai, M. Werner, Shunt types in crystalline silicon solar cells, Prog. Photovolt: Res. Appl. 12 (2004) 529.
[5] M.H. Al Rifai, O. Breitenstein, J.P. Rakotoniaina, M. Werner, A. Kaminski, N.L. Quang, Investigations of material–induced-shunts in block–cast multicrystalline silicon solar cells caused by SiC precipitate filaments, in: Proceedings of the 19th European Photovoltaic Solar Energy Conference and Exhibition, Paris, France, 2004, pp. 632–635.
[6] J.P. Rakotoniaina, O. Breitenstein, M. Werner, M.H. Al Rifai, T. Buonassisi, M.D. Pickett, M. Ghosh, A. Müller, N.L. Quang, Distribution and formation of silicon carbide and silicon nitride precipitates in block–cast multicrystalline silicon, in: Proceedings of the 20th European Photovoltaic Solar Energy Conference and Exhibition, Barcelona, Spain, 2005, pp. 773–776.
[7] O. Breitenstein, J. Bauer, J.P. Rakotoniaina, Material-induced shunts in multicrystalline silicon solar cells, Semiconductors 41 (2007) 440.
[8] J. Bauer, O. Breitenstein, J.P. Rakotoniaina, Electronic activity of SiC precipitates in multicrystalline solar silicon, Phys. Stat. Sol. (a) 204 (2007) 2190.
[9] G. Du, L. Zhou, P. Rossetto, Y. Wan, Hard inclusions and their detrimental effects on the wire sawing process of multicrystalline silicon, Sol. Energy Mater. Sol. Cells 91 (2007) 1743.
[10] A.-K. Søiland, E.J. Øvrelid, T.A. Engh, O. Lohne, J.K. Tuset, Ø. Gjerstadt, SiC and Si_3N_4 inclusions in multicrystalline silicon ingots, Mater. Sci. Semicond. Process. 7 (2004) 39.
[11] A.-K. Søiland, Silicon for solar cells, Ph.D. Thesis, Department of Materials Technology, Norwegian University of Science and Technology (NTUN), Trondheim, Norway, 2004.
[12] R. Zhang, E.E. van Dyk, G.A. Rozgonyi, J. Rand, R. Jonczyk, Investigation of foreign particles in polycrystalline silicon using infrared microscopy, Sol. Energy Mater. Sol. Cells 82 (2004) 577.
[13] J. Bauer, O. Breitenstein, A. Lotnyk, H. Blumtritt, Investigations on different types of filaments in multi–crystalline silicon for solar cells, in: Proceedings of the 22nd European Photovoltaic Solar Energy Conference and Exhibition, Milano, Italy, 2007, pp. 994–997.
[14] S. Nakahara, Recent development in a TEM specimen preparation technique using FIB for semiconductor devices, Surf. Coat. Technol. 169–170 (2003) 721.
[15] R.W.G. Wyckoff, Crystal Structures, vol. 1, Wiley/Interscience, New York, 1963.
[16] H. Bender, A. Veirman, J. Landuyt, S. Amelinckx, HREM investigation of twinning in very high dose phosphorus ion–implanted silicon, Appl. Phys. A 39 (1986) 83.
[17] U. Kaiser, A. Chuvilin, P.D. Brown, W. Richter, Origin of threefold periodicity in high–resolution transmission electron microscopy images of thin film cubic SiC, Microsc. Microanal. 5 (1999) 420.
[18] M.W. Chase (Ed.), NIST–JANAF Thermochemical Tables, American Institute of Physics, Woodbary, NY, 1998.
[19] V. Heine, C. Cheng, R.J. Needs, The preference of silicon carbide for growth in the metastable cubic form, J. Am. Ceram. Soc. 74 (1991) 2630.
[20] J. Bauer, J.O. Breitenstein, M. Becker , J. Lenzner, Electrical investigations on SiC precipitates found in block–cast solar silicon, in Proceedings of the Seventh NREL Workshop on Crystalline Silicon Solar Cells and Modules: Materials and Processes, Vail, USA, 2007, pp. 233–236.
[21] F. Shmidt, C.P. Khattak, T.G. Digges, L. Kaufman, Origin of SiC impurities in silicon crystals grown from the melt in vacuum, J. Electrochem. Soc. 126 (1979) 935.
[22] K.S. Nahm, K.C. Kim, K.Y. Lim, Growth and characterization of $SiC/SiN_x/Si$ structures, J. Electrochem. Soc. 148 (1998) G132.
[23] R.W. Cahn, P. Haasen (Eds.), Physical Metallurgy, North-Holland Physics Publishing, 1983.
[24] O. Breitenstein, M. Langenkamp, Quantitative local analysis of I–V characteristics of solar cells by thermal methods, in: Proceedings of the Second World Conference and Exhibition on Photovoltaic Solar Energy Conference and Exhibition, Vienna, Austria, 1998, pp. 1382–1385.